

Harmonic Distortion In The Flow Signals Of Externally Mounted Capacitive Spatial Filter

Marwa Malik Hassooni

Department of Electronic and
Communication Engineering
Coll. of Eng., Al-Nahrain University
elea_mm313@yahoo.com

Abbas Ahmad Al Shalchi

Department of Electronic and
Communication Engineering
Coll. of Eng., Al-Nahrain University

Abstract

This paper investigates the performance of some windows on the flow signals that are generated from the planar capacitance spatial filter (PCSF) according to the moving of the solid particle in the channel of the filter. The finite-difference equations are solved using successive over relaxation (SOR) methods, The waveforms show that the response of the PCSF is spatially-biased towards particle flowing closer to the plane of sensing electrodes and that the resulting flow signal is non-sinusoidal. The total harmonic distortion (THD) content on the flow signals are calculated with respect to the fundamental frequency of the power spectrum density through a specific quantitative criterion. This paper comprises a comparative study among three types of windows; Hanning, Hamming, and a suboptimal window called the Kaiser window. The effect of particle flying heights and relative permittivity on the THD of the flow signal was examined.

Keywords: Hanning; Hamming; Kaiser; Window; Total harmonic distortion

1 Introduction

Mass flow rate and concentration measurement are important factors in many industries such as coal fired power plants, pharmaceutical, chemical and food stuff production processes. Control of flow parameters effectively improves productivity, product quality and process efficiency in such industries [1]. Mass flow measurement methods are categorized in two groups, inferential measurement methods and direct or true measurement methods. In inferential measurement, particles mass flow rate is obtained by measuring and multiplying of instantaneous velocity and concentration [2]. Installing the proper measurement system depends on nature of particles flow in the pneumatic conveyors, material type and particle's size, velocity, moisture and homogeneity profile. There are

many flow sensing techniques in indirect methods for measuring volumetric concentration and velocity of solids. They are based on: capacitance sensors, electrostatic sensors and spatial filters [3], which are electrical sensors, whereas radiometric sensors [4], acoustic sensors, laser Doppler Velocimeters (LDV) and optical sensors [5] are attenuation and scattering methods [6]. Electrical capacitance tomography (ECT) and electrical optical tomography (EOT) are tomographic methods[7]. The direct approach is a more straightforward way compared with (inferential) measurement. It is based on Coriolis force and thermal methods[8].

2 The Space-Periodic Capacitance Transducer (SPCT)

The multi-electrode capacitance transducer (MECT) or the space periodic capacitance transducer (SPCT) with periodic electrode structure, is one type of indirect measurements spatial filter. Space Periodic Capacitance Transducer (SPCT) has pairs of electrodes arranged on opposite sides of a flow channel in a parallel-plate arrangement which responds to permittivity changes over the whole cross-section of the flow, although the inevitable non-uniformity of the field means that the flow in some regions of channel contributes more to the capacitance variation than in others. Furthermore, the large separation between the electrodes means that capacitance variations are small unless electrodes of appreciable length are used. In the space-periodic arrangement which is the basis of the present method, there is, furthermore, considerable capacitance between neighbouring electrodes along each channel wall [9].

An alternative arrangement is to use a larger number of smaller and more closely spaced electrodes on one side of the channel only as shown in fig.(1).

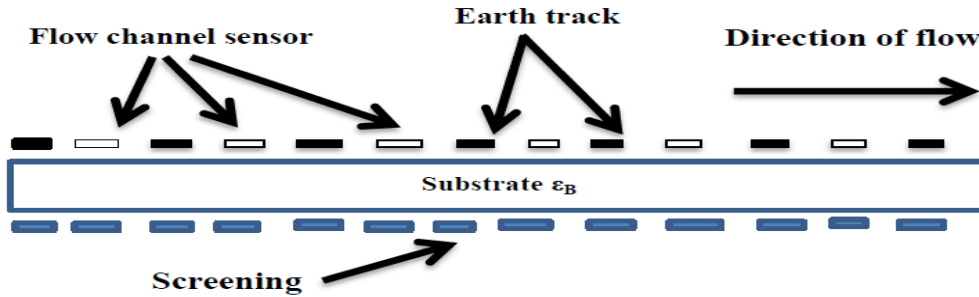


Figure 1: Cross section of the PCST

3 Geometrical Model

The transducer consists of two interlacing combs of conducting electrodes and a third continuous earthed track which separates the electrodes of the two combs. The arrangement is shown in plan view in fig.(1). The combs constitute the sensor electrodes and are connected through capacitance-to-voltage convertor circuits to the two inputs of a differential amplifier. Six sensors are included in each comb, each sensor being 1 mm wide and separated by 1 mm from the earthed electrode on each side of it. The screening electrodes are deposited on the reverse side of the substrate and connected to the sensors through voltage followers. Simulation of one cell of the finite SPCT represents the simulation of the complete system. This is true because all the six interlaced sensors can be sectioned into a number of identical cells [9]. The SOR algorithm was used to find the potential distribution inside the cell by first covering the cell by a mesh with a space h_x between each consecutive point in the direction of x-axis and h_y in the direction of y-axis and locating the boundary conditions. Initial conditions for these boundaries are required to start the SOR in its iterative loop. The width of

one cell is set to be 4mm, height is 20mm, substrate thickness (t) is 0.901mm ($5h_y$) [10].

4 Effects of the Windows on the Flow Signals

The Incremental capacitance waveforms are presented in fig.(2) for the case of a particle passing close to the shielded sensors at altitude of $d=0.2t$ have sharp points these are undesirable owing to their high harmonic content. Also some of these signals(from particles close to the sensors plane) suffer from the presence of half cycle secondary lobes and half cycle cavity or dip problems which are undesirable. Weighing windows have been suggested so as to cut the error that non coherent sampling induces in the measurement of a power and harmonic parameters. The signal becomes enriched with unwanted harmonics, the largest of them being the one with double the fundamental frequency. It is therefore necessary to choose the existing, or to synthesize new, specialized windows that would suppress harmonics. Fig.(3) to (5) show the windowing of the incremental capacitance for the relative permittivity of the particle of 100 by Hamming, Hanning and Kaiser windows of a particle flying heights $d=1h_y$ to $8h_y$.

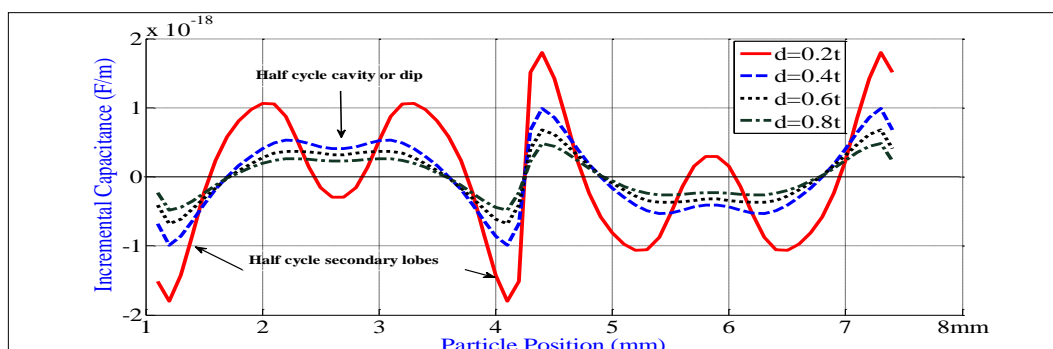


Figure 2: Incremental capacitance waveform of the two cells for shielding layer having $\epsilon_s=4$, $\epsilon_p = 100$, $t = 5h_y$ with particle flying heights $d=0.2$ to $0.8t$

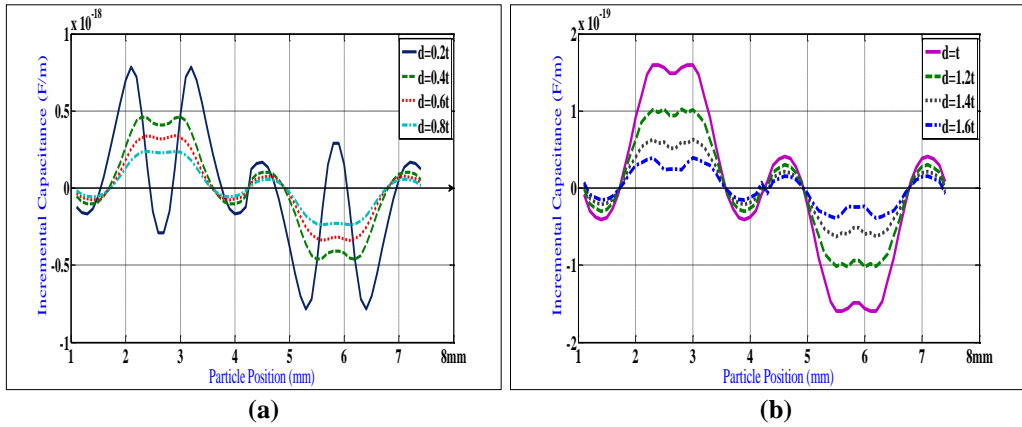


Figure 3: Windowing the flow signal for a particle relative permittivity 100 by the Hamming window (a) particle flying heights $d=0.2t$ to $0.8t$ (b) particle flying heights $d=t$ to $1.6t$

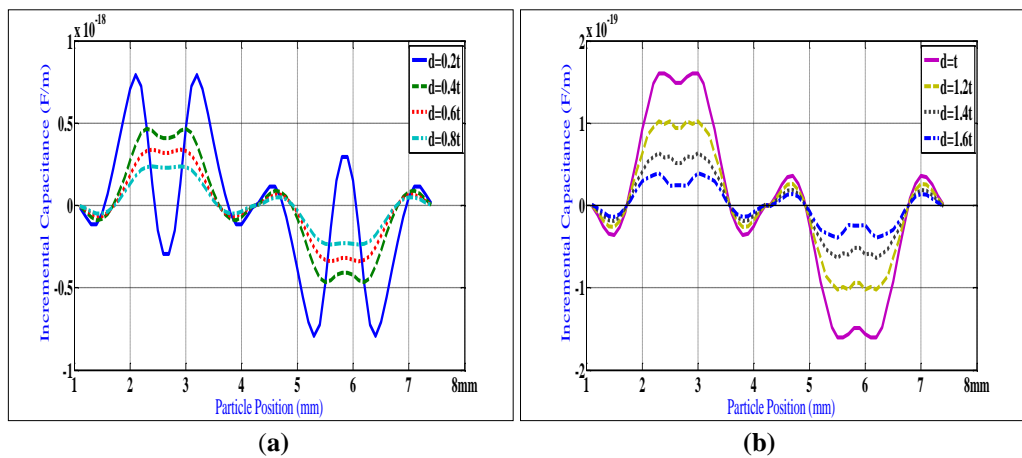


Figure 4: Windowing the flow signal for a particle permittivity of 100 by the Hanning window (a) particle flying heights $d=0.2t$ to $0.8t$ (b) particle flying heights $d=t$ to $1.6t$

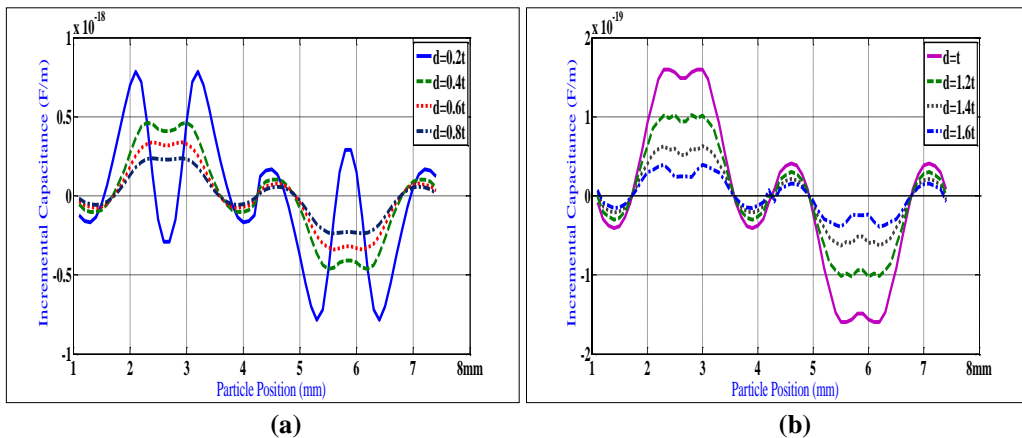


Figure 5: Windowing the flow signal for a particle relative permittivity 100 by the Kaiser window (a) particle flying heights $d=0.2t$ to $0.8t$ (b) particle flying heights $d=t$ to $1.6t$

5 Total Harmonic Distortion

Harmonic distortion can be caused by both active and passive non-linear devices in a power system. The power transformer, for example, generates a magnetization current with third-order and higher odd harmonics. In the past, these passive devices were the primary source of

harmonics. Today, most harmonic distortion is generated by input stage of (active) electronic power converters [11]. However, when broken down into the basic definitions of harmonics and distortion, it becomes much easier to understand.

In an ideal power system, the voltage supplied to customer equipment, and the resulting load current are perfect sine waves. In practice, however, conditions are never ideal, so these waveforms are often quite distorted. This deviation from perfect sinusoids is usually expressed in terms of harmonic distortion of the voltage and current waveforms.

Thus, harmonic distortion is the degree to which a waveform deviates from its pure sinusoidal values as a result of the summation of all these harmonic elements.

$$THD = \frac{\sqrt{\sum_{n=2}^{\infty} X_n^2}}{X_1} * 100\% \quad \dots(1)$$

The formula above shows the calculation for total harmonic distortion THD of a signal, where X_1 is the fundamental component and X_n are other harmonic components. Total harmonic distortion, or THD, is the summation of all harmonic components of the voltage or current waveform compared against the fundamental component of the voltage or current wave [12].

5.1 Effect of the Particle Heights on the THD

Fig.(6) shows the total harmonic distortion of the flow signals when particle relative permittivity is 100. The values of the harmonic distortion of the flow signals were measured for particle flying heights from $d=0.2t$ to $d=1.6t$ and are shown in Table (1) when particle relative permittivity is 50, of each particle height, the sub optimal window (Kaiser window) suppressing the harmonic of the flow signals more than the other two, and it can be seen that the behavior of Hanning and Hamming windows appears roughly the same in suppressing the HD.

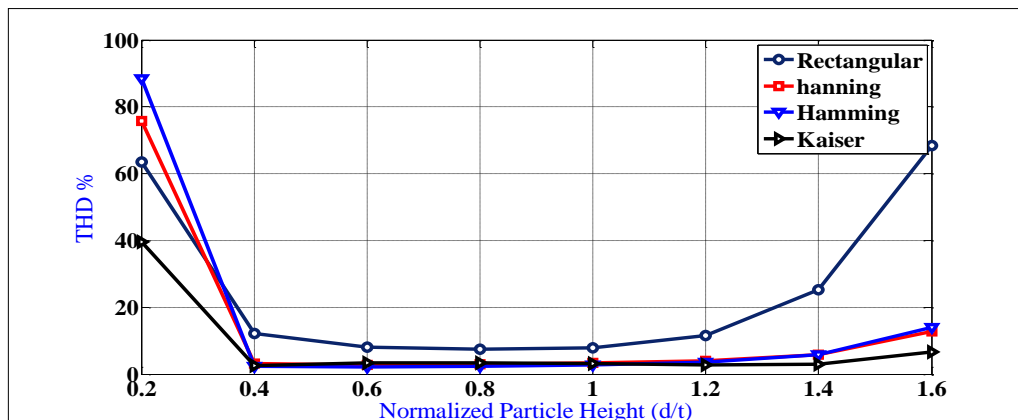


Figure 6: Total Harmonic Distortion of the flow signals vs. normalized particle flying height for particle relative permittivity $\epsilon_p=100$

Table 1: Total Harmonic Distortion of the flow signal for the particle relative permittivity $\epsilon_p=50$

Particle Height(d)	THD% (Rectangular window)	THD% (Hanning window)	THD% (Hamming window)	THD% (Kaiser window)
0.2t	79.153	53.174	60.299	32.176
0.4t	11.763	3.0037	2.2612	2.657
0.6t	7.843	2.781	2.0231	3.5867
0.8t	6.5106	2.8829	2.1716	3.7655
t	7.1006	3.1865	2.5992	3.4429
1.2t	15.912	2.5108	1.8217	2.0519
1.4t	18.852	4.9985	4.9102	2.93
1.6t	49.355	8.4596	9.1542	3.9391

5.2 Effect of Particle Permittivity on the THD

In the previous sections the effects of the particle flying heights on the total harmonic distortion is noted. It is affected by the windows that are used in the two cases when a particle has relative permittivity of 100 and half of this value. Now to do comprehensive examination of the effects of particle parameters on the total harmonic distortion in this section, two specific flying heights of a particle are chosen and in

each one of these heights the particle relative permittivity will be changed in nine steps from 10 to 90.

Table (2) displays the values of the THD of the flow signal for each particle permittivity when the choosed particle height (d) is 1.2 t. Fig. (7) shows of the total harmonic distortion when the particle fly at the height 0.6t (close to the sensor line).

Table 2: The THD of a flow signal for various particle permittivity for height d= 1.2t

Particle relative Permittivity(ϵ_p)	THD% (Rectangular window)	THD% (Hanning window)	THD% (Hamming window)	THD% (Kaiser window)
10	4.2163	3.5763	2.7954	5.2504
20	6.459	3.2138	2.6231	3.9925
30	7.8653	3.3671	2.869	3.5357
40	8.8477	3.5758	3.1307	3.275
50	9.4154	3.6685	3.2509	3.1844
60	9.8861	3.7735	3.3764	3.1046
70	10.246	3.8566	3.4743	3.0509
80	10.528	3.9213	3.5501	3.0134
90	10.759	3.9782	3.6157	2.9847

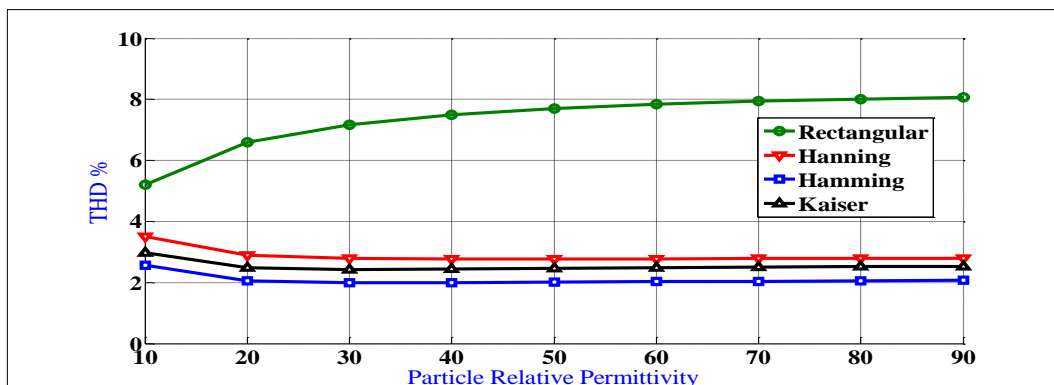


Figure 7: Total Harmonic Distortion of the flow signals vs. particle relative permittivity for a particle flying height (d) =0.6t

Conclusions

In this work some important characteristics of the planar capacitance spatial filter (PCSF) are investigated by using MATLAB language. The flow signals at a particle size of $(2h_x \times 2h_y)$ are studied. The waveforms of the incremental capacitance are confirmed to be non-sinusoidal and generally have power leakage and harmonics.

The particle parameters include flying height and permittivity were investigated. In this work some well-known windows have been used to smooth the flow signals. They are mainly others, and the THD becomes stable at the remaining heights, but if we fix two of particle heights at 0.6t and 1.2t during each one, the permittivity changes nine times the values of the THD giving new reading around 4%, 3%, and 2% surely after the Hamming, the Hanning and the Kaiser windows respectively.

Hanning, Hamming and Kaiser windows. The Hannnig window is important due to its side-lobe falloff, on the same time the Kaiser window gives better sidelobe reduction as seen in the graphgs.

The total harmonic distortion (represented in percentage %THD) is calculated with respect to the fundamental frequency for a particle relative permittivity of 100 and 50 with eight flying heights, the values of the THD for the height near the sensor show more distortion than

References

[1] Yan, Y. Xu, Y. Lee, P. (2006), "Mass Flow Measurement of Fine Particles in a Pneumatic Suspension Using Electrostatic Sensing and Neural Network Technique", IMTC 2005-

- Instrumentation and Measurement, Vol. 1, pp. 2330-2334.
- [2] Beck, M., S., Green, R. G., Thorn, R., (1987), "Non-Intrusive Measurement of Solids Mass Flow in Pneumatic Conveying", J. Phys. E: Sci. Instrum. Vol. 20, pp. 835-840.
- [3] Xu, C., Tang, G., Zhou, B., Zhou, S., (2009), "The Spatial Filtering Method for Solid Particle Velocity Measurement Based on an Electrostatic Sensor " Measurement Science and Technology, vol. 20, No. 3, pp.1-8.
- [4] Barratt, I., R., Yan, Y., Byrne, B., (2001), "A Parallel-Beam Radiometric Instrumentation System for the Mass Flow Measurement of Pneumatically Conveyed Solids", Measurement Science and Technology ,vol. 12, No. 9 , pp.1515-1528.
- [5] Sun, M., Liu, S., Lei, J., Li , Z., (2008), "Mass Flow Measurement of Pneumatically Conveyed Solids Using Electrical Capacitance Tomography", Measurement Science and Technology , vol. 19, No.4, pp.1-6.
- [6] Jaworski, A., J., Dyakowski, T., (2001), "Application of Electrical Capacitance Tomography for Measurement of Gas-Solids Flow Characteristics in a Pneumatic Conveying System", Measurement Science and Technology ,vol.12, No. 9, pp. 1109-1119.
- [7] Song, D., Peng, L., Lu, G., Yang, S., Yan, Y., (2009), "Digital Image Processing Based Mass Flow rate Measurement of Gas/Solid Two-Phase Flow ", in The 6th International Symposium on Measurement Techniques for Multiphase Flows, Journal of Physics: Conference Series, vol. 147, No.1, pp. 1-8.
- [8] Zheng, Y., Pugh, J., McGlinchey, D., Knight, E., (2009), "Investigation of Heat Transfer Coefficient in Gas-Solids Dense Phase Pneumatic Pipe Flow, Bulk Solids & Powder Science & Technology, vol. 4, No. 4, pp. 169-174.
- [9] Deeley, E., M., Al-Shalchi, A., (1982), "Space Periodic Capacitance Transducer for the Measurement of Flow Velocity" , IEE proc.-D(GB), vol.129, No. 4, pp.105-112, July.
- [10] Abbas, N., I., (1990), "Modeling of Finite Length Space Periodic Capacitance Transducer Using Difference Methods", M.Sc. dissertation ,University of Technology, Baghdad, Iraq, Sep.
- [11] Vlahinica, S., Brnobica, D., Vucetic, D., (2009), "Measurement and Analysis of Harmonic Distortion in Power Distribution Systems ", Electric Power Systems Research 79, pp. 1121-1126.
- [12] Sathit, E., J., (2012), "Optimal Technique for Total Harmonic Distortion Detection and Estimation for Smart Meter ", King Mongkut's Institute of Technology Ladkrabang (KMITL), Bangkok, Thailand IEEE

التشوه بالتوافقيات في اشارات التدفق للمتحمس السعوي الحيزي المثبت خارجيا

عباس احمد الشالحي
هندسة الألكترونيك والاتصالات
كلية الهندسة - جامعة النهريين

مروه مالك حسوني
هندسة الألكترونيك والاتصالات
كلية الهندسة - جامعة النهريين

الخلاصة

تتحرى المقالة في أداء بعض أنواع النوافذ على الإشارات المتدفقة المتولدة من المرشح السعوي الحيزي المستوي (SCPF) وفقاً لحركة الجسيمة الصلبة في قناة المرشح. معادلات الفروقات المتناهية حُلت باستخدام طرق تقنيّة التراخي المفرط المتتابع (SOR) , وإن أشكال الموجات المستحصلة تُبين إن استجابة (PCSF) متحيزه مكانياً نحو تدفق الجسيمة القريبة من مستوي أقطاب المتحمس, وإن الإشارة المتدفقة الناتجة ليست جيبيّة. تشويه التوافقيات الكلي (THD) المحتوى في اشارات التدفق حُسب بالنسبة للتردد الاساسي لكثافة الطيف الكهربائيّة خلال معيار كمي خاص محدد, هذا المقال يشمل دراسة مقارنه بين ثلاث أنواع من النوافذ (Hanning, Hamming) والنافذه الشبه مثاليه والتي تسمى نافذة كايزر (Kaiser). تم إختبار تأثير إرتفاع طيران الجسيمة و سماحيته النسبية على التشويه التوافقي الكلي (THD) لإشارة التدفق.